

# On the Shape of a Cable Towed in a Circular Path

RICHARD A. SKOP

*Ocean Structures Branch  
Ocean Technology Division*

April 24, 1970



**NAVAL RESEARCH LABORATORY**  
**Washington, D.C.**

This document has been approved for public release and sale; its distribution is unlimited.

## DOCUMENT CONTROL DATA - R &amp; D

(Security classification of title, body of abstract and indexing annotation must be entered when the overall report is classified)

1. ORIGINATING ACTIVITY (Corporate author) Naval Research Laboratory Washington, D. C. 20390		2a. REPORT SECURITY CLASSIFICATION Unclassified	
3. REPORT TITLE  ON THE SHAPE OF A CABLE TOWED IN A CIRCULAR PATH		2b. GROUP	
4. DESCRIPTIVE NOTES (Type of report and inclusive dates) An interim report on one phase of a continuing problem.			
5. AUTHOR(S) (First name, middle initial, last name)  Richard A. Skop			
6. REPORT DATE April 24, 1970		7a. TOTAL NO. OF PAGES 32	7b. NO. OF REFS 10
8a. CONTRACT OR GRANT NO. F02-24		9a. ORIGINATOR'S REPORT NUMBER(S) NRL Report 7048	
b. PROJECT NO. RR 009-03-45-5807		9b. OTHER REPORT NO(S) (Any other numbers that may be assigned this report)	
c.		d.	
10. DISTRIBUTION STATEMENT  This document has been approved for public release and sale; its distribution is unlimited.			
11. SUPPLEMENTARY NOTES		12. SPONSORING MILITARY ACTIVITY Department of the Navy (Office of Naval Research), Washington, D.C. 20360	
13. ABSTRACT  The problem of determining the shape of a cable towed in a circular path is considered both by experimental and theoretical techniques. The equations of static equilibrium, referred to a rotating coordinate system, are derived and nondimensionalized to isolate the important parameters. Certain order-of-magnitude simplifications are obtained. The remainder of the study is restricted to cases where the effect of hydrodynamic drag is negligible. The experimental results indicate that for certain combinations of the governing parameters no stable equilibrium solution for the cable shape exists. Rather, at these combinations, the system is marked by a violent dynamic motion between two adjoining nodal configurations. To examine this phenomenon analytically, the static equations are idealized to a vacuous towing medium. It is shown that these equations possess several possible solutions. The questions of stability of equilibrium and onset of transition are resolved from these solutions by reference to the experimental observations. Since no drag forces are present in a vacuum, it is concluded that the centrifugal loading is the principal agent responsible for producing the unsteady dynamic behavior of the cable.			

14. KEY WORDS	LINK A		LINK B		LINK C	
	ROLE	WT	ROLE	WT	ROLE	WT
Cables Cable analysis Cable towed in a circular path Instabilities of circularly towed cables Shape of circularly towed cables						

## CONTENTS

Abstract	ii
Problem Status	ii
Authorization	ii
SYMBOLS	1
Symbols Appearing in Dimensional Equations	1
Symbols Appearing in Nondimensional Equations	2
INTRODUCTION	3
EQUATIONS OF EQUILIBRIUM	4
THE EXTERNAL FORCE ON THE CABLE	5
THE EXTERNAL FORCE ON THE FISH	6
A NONDIMENSIONAL FORM OF THE EQUILIBRIUM EQUATIONS	7
A DISCUSSION OF THE NONDIMENSIONAL PARAMETERS	9
RESULTANT FORCE TRANSFORMATION AND THE EQUILIBRIUM EQUATIONS IN COMPONENT FORM	10
SOME EMPIRICAL RESULTS	12
ON THE SHAPE IN A VACUUM	15
METHOD OF SOLUTION	17
THE CHARACTER OF THE SOLUTIONS FOR $\lambda \leq \lambda_c$ (ZERO-NODE SOLUTIONS)	19
THE CHARACTER OF THE SOLUTIONS FOR $\lambda > \lambda_c$ (NODAL SOLUTIONS)	21
SOME QUALITATIVE CONSIDERATIONS	25
CONCLUSIONS	26
ACKNOWLEDGMENTS	27
REFERENCES	27

## ABSTRACT

The problem of determining the shape of a cable towed in a circular path is considered both by experimental and theoretical techniques. The equations of static equilibrium, referred to a rotating coordinate system, are derived and nondimensionalized to isolate the important parameters. Certain order-of-magnitude simplifications are obtained. The remainder of the study is restricted to cases where the effect of hydrodynamic drag is negligible. The experimental results indicate that for certain combinations of the governing parameters no stable equilibrium solution for the cable shape exists. Rather, at these combinations, the system is marked by a violent dynamic motion between two adjoining nodal configurations. To examine this phenomenon analytically, the static equations are idealized to a vacuous towing medium. It is shown that these equations possess several possible solutions. The questions of stability of equilibrium and onset of transition are resolved from these solutions by reference to the experimental observations. Since no drag forces are present in a vacuum, it is concluded that the centrifugal loading is the principal agent responsible for producing the unsteady dynamic behavior of the cable.

## PROBLEM STATUS

This is an interim report; work is continuing on other phases of the problem.

## AUTHORIZATION

NRL Problem F02-24  
Project RR-009-03-45-5807

Manuscript submitted January 6, 1970.

## ON THE SHAPE OF A CABLE TOWED IN A CIRCULAR PATH

### SYMBOLS

The symbols used in this report are defined as they appear in the text. The most important ones are listed here for reference.

#### Symbols Appearing in Dimensional Equations

$a$	the acceleration of the cable as seen by the fluid
$A$	the cross-sectional area of the cable
$A_f$	the cross-sectional area to which drag on the fish is referenced
$C_D$	the drag coefficient of the cable
$C_{Df}$	the drag coefficient of the fish
$d$	the diameter of the cable
$f$	the external load per unit length on the cable
$f_a, f_c, f_h, f_w$	respectively, the apparent mass force, the centrifugal force, the hydrodynamic force, and the weight force, all per unit length, acting on the cable
$F_f$	the external load on the fish
$F_{fa}, F_{fc}, F_{fh}, F_{fw}$	respectively, the apparent mass force, the centrifugal force, the hydrodynamic force, and the weight force acting on the fish
$g$	the constant of gravitational acceleration
$i, j, k$	respectively, unit vectors along the $X$ , $Y$ , and $Z$ axes
$L$	the length of the cable
$M$	the mass of the fish
$M'$	the appropriate component of the apparent mass tensor of the fish due to its radial acceleration through the fluid
$P$	the position vector of a point on the cable
$P_f$	the position vector of the fish
$R$	the radius of the circle along which the towpoint of the cable moves

$S$	the arc length measured along the cable
$\tilde{T}$	the tension at a point along the cable
$V$	the speed with which the towpoint of the cable moves
$v$	the velocity of the cable as seen by the fluid
$v_n$	the component of $v$ which is normal to the cable
$V_f$	the velocity of the fish as seen by the fluid
$W$	the weight of the fish
$W'$	the weight of the fluid displaced by the fish
$X, Y, Z$	the axes of a rotating, right-handed, Cartesian coordinate system
$\mu$	the mass per unit length of the cable
$\rho$	the mass density of the fluid
$\Omega$	the rotational frequency of the rotating coordinate system = $V/R$
$\Omega$	the vector angular velocity of the rotating coordinate system = $\Omega k$

#### Symbols Appearing in Nondimensional Equations

$C$	the drag constant of the cable = $(1/2) \rho C_D dR / (\mu + \rho A)$
$C_f$	the drag constant of the fish = $(1/2) \rho C_{Df} A_f / (\mu + \rho A)$
$E(\lambda)$	an error function
$m_f$	the nondimensional mass of the fish = $(M + M') / [(\mu + \rho A) R]$
$p$	the nondimensional position vector of a point on the cable = $P/R$
$R$	the nondimensional resultant force vector = $T \frac{dp}{ds}$
$R_x, R_y, R_z$	the components of $R$
$R_{x0}$	the value of $R_x$ at $s = 0$
$R_{x0}^{cn}(\lambda, C, w_f)$	the value of $R_{x0}$ immediately following transition of the cable to its $n$ th nodal shape
$R_{x0}^{cn}(\lambda, w_f)$	an abbreviated notation for $R_{x0}^{cn}(\lambda, C, w_f)$ when $C = 0$
$s$	the nondimensional arc length measured along the cable = $S/R$
$T$	the nondimensional tension at a point along the cable = $\tilde{T} / [(\mu + \rho A) gR]$

$v_n^*$	the nondimensional normal velocity of the cable through the fluid = $v_n/V$
$w$	the nondimensional weight of the cable = $(\mu - \rho A)/(\mu + \rho A)$
$w_f$	the nondimensional weight of the fish = $(W - W')/[(\mu + \rho A)gR]$
$x, y, z$	the nondimensional axes of a rotating, right-handed Cartesian coordinate system = $X/R, Y/R, Z/R$ , respectively
$\gamma$	the nondimensional rotational frequency = $\Omega \sqrt{R/g} = V/\sqrt{Rg}$
$\gamma_{cn}(\lambda, C, w_f)$	the value of $\gamma$ at which transition of the cable to its $n$ th nodal shape occurs
$\gamma_{cn}(\lambda, w_f)$	an abbreviated notation for $\gamma_{cn}(\lambda, C, w_f)$ when $C = 0$
$\lambda$	the nondimensional length of the cable = $L/R$
$\lambda_c$	the value of $\lambda$ below which only zero-node cable shapes are possible

## INTRODUCTION

With the work of Pode (1), Wilson (2), and Skop and O'Hara (3), the quasi-static problem of determining the shape of a flexible, extensible cable towed in a straight path has been well resolved for a large variety of hydrodynamic loadings. The remaining outstanding quasi-static question concerns the shape of a cable towed in a circular path. A recent bibliographic survey (4) of studies on the configurations of cable systems indicates that little, if any, work has been done on the circular towing problem.

Aside from its theoretical interest, this problem has practical significance because, for certain combinations of the governing parameters, the free end of the cable takes a position at a given depth below the center of the towing circle. Thus, the possible use of the circular towing concept for an intensive search or photographic mission of a particular area is of interest.

This report considers, both by experimental and theoretical means, the shape of a flexible, inextensible cable towed in a circular path. The equations of equilibrium and the boundary conditions which govern the cable shape are derived and nondimensionalized to isolate the important parameters. A discussion of these parameters follows, and certain order-of-magnitude simplifications are obtained.

Even with these simplifications, the governing equations are still quite complex; therefore, to determine some parametric values for which the free end of the cable is stationary below the center of the towing circle, an experiment was performed. The results of this experiment showed many unexpected phenomena, of which the most important is that for certain combinations of parameters no static solution for the cable shape is possible.

Obviously, the static equilibrium equations cannot be used to study the dynamic behavior of the cable. This does not, however, negate their validity for predicting the onset of unstable behavior and for determining the cable shape when static solutions are possible. To ascertain whether the theoretical equations possess these properties, the numerical studies in this report have been restricted to determining the cable shape in a

vacuum. This restriction is in accord with the reported experiment for which the effect of drag was negligible.

The assumption of a vacuous medium reduces the equilibrium problem from a highly intractable set of six first-order, nonlinear differential equations to a set of two first-order, nonlinear differential equations. Meanwhile, this assumption maintains the basic characteristic which distinguishes towing in a circle from towing in a straight line. This is the presence of a centrifugal force acting on the cable.

The results of this study clearly show that, with the proper interpretation, the equilibrium equations are fully capable of predicting both the static cable shape and the onset of cable instability.

### EQUATIONS OF EQUILIBRIUM

Let  $X$ ,  $Y$ , and  $Z$  be the axes of a rotating, right-handed, Cartesian coordinate system (Fig. 1), the origin of which coincides with the center of a circle of radius  $R$  along which a ship moves with speed  $V$ . The  $Z$  axis is specified as the axis of rotation.  $Z = 0$  is taken as the water surface, and  $Z$  is considered as increasing down into the water. The  $X$  axis of this system rotates along with the ship. The unit vectors along the  $X$ ,  $Y$ , and  $Z$  axes are represented by  $i$ ,  $j$ , and  $k$ , respectively.

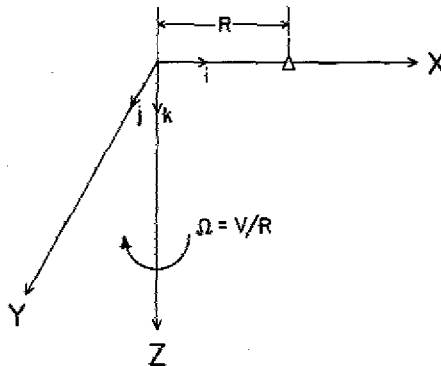


Fig. 1 - Rotating Cartesian coordinate system

If the position vector of a point on the cable is denoted by  $P$ , where

$$P = Xi + Yj + Zk, \quad (1)$$

then the equations of equilibrium for a flexible, inextensible cable are given by

$$\frac{d}{dS} \left( \tilde{T} \frac{dP}{dS} \right) + f = 0, \quad (2a)$$

where  $\tilde{T}$  is the tension in the cable,  $f$  is the external load per unit length, and  $S$  is the arc length measured along the cable. To the equations of equilibrium must be added the geometric constraint

$$\sqrt{\frac{dP}{dS} \cdot \frac{dP}{dS}} = 1. \quad (2b)$$

If  $S$  is taken as zero at the ship and as  $L$  at the towed body (fish), the appropriate boundary conditions for the problem are

$$\mathbf{P}|_{S=0} = R \mathbf{i} \quad (3a)$$

and

$$\left( \tilde{T} \frac{d\mathbf{P}}{dS} \right) \Big|_{S=L} = \mathbf{F}_f \quad (3b)$$

In Eq. (3b),  $F_f$  denotes the external force acting on the fish. The expression for this force will be considered presently.

#### THE EXTERNAL FORCE ON THE CABLE

The external force per unit length  $\mathbf{f}$  acting on the cable can be resolved into four parts: gravity and buoyancy forces, centrifugal forces, apparent mass forces, and hydrodynamic drag forces.

If the linear density (mass per unit length) of the cable is given as  $\mu$ , then the gravitational force per unit length is  $\mu g \mathbf{k}$ , where  $g$  is the gravitational acceleration. Also, applying Archimedes' principle, the buoyancy force per unit length can be written as  $-\rho A g \mathbf{k}$ , where  $A$  is the cross-sectional cable area and  $\rho$  is the mass density of the water. The gravity and buoyancy forces can be combined into one weight force given by

$$\mathbf{f}_w = (\mu - \rho A) g \mathbf{k} \quad (4)$$

Before deriving the centrifugal, apparent mass, and hydrodynamic forces, it is necessary to determine the velocity and acceleration of the cable as seen by the water, which is at rest. Since the coordinate system is rotating with the ship about the  $Z$  axis, the vector angular velocity  $\Omega$  of the system is given by

$$\Omega = \Omega \mathbf{k} \quad (5a)$$

where the rotational frequency  $\Omega$  is

$$\Omega = V/R \quad (5b)$$

To obtain the proper sign for  $\Omega$ ,  $V$  must be taken as positive if the center of the towing circle remains to the starboard of the ship. On remembering, that in equilibrium, the cable has no motion relative to the rotating coordinate system, the velocity  $\mathbf{v}$  and the centripetal acceleration  $\mathbf{a}$  as seen by the water of the cable point  $\mathbf{P}$  are found from Coriolis' theorems as

$$\mathbf{v} = \Omega \times \mathbf{P} = \Omega \mathbf{k} \times \mathbf{P} \quad (6a)$$

and

$$\mathbf{a} = \Omega \times (\Omega \times \mathbf{P}) = \Omega^2 \mathbf{k} \times (\mathbf{k} \times \mathbf{P}) \quad (6b)$$

As is well known, the centripetal acceleration leads to the presence of a centrifugal force per unit length  $\mathbf{f}_c$ . This force is equal in magnitude to  $\mu \mathbf{a}$  but acts in the opposite direction; consequently, from Eq. (6b),

$$\mathbf{f}_c = -\mu \Omega^2 \mathbf{k} \times (\mathbf{k} \times \mathbf{P}) \quad (7)$$

The centripetal acceleration also leads to the presence of apparent mass forces on the cable. Since a cable can be approximated as a circular cylinder, the apparent mass force per unit length  $f_a$  can be obtained from Lamb (5) as  $-\rho A a$ . Again from Eq. (6b), the apparent mass force becomes

$$f_a = -\rho A \Omega^2 \mathbf{k} \times (\mathbf{k} \times \mathbf{P}) . \quad (8)$$

Consider now the hydrodynamic drag force. The usual method of specifying this force (6) is to resolve it into components along three mutually perpendicular directions known as the hydrodynamic axes. These three directions are, respectively, parallel to the component of relative velocity which is tangent to the cable, parallel to the component of relative velocity which is normal to the cable, and parallel to the direction which is mutually orthogonal to the former two directions. In this coordinate system, the components of the hydrodynamic force are known, respectively, as the tangential drag, the normal drag, and the side drag. The relative velocity is the total velocity of the cable as seen in the rest frame of the fluid. Since, for the problem under consideration, the fluid is already at rest, the relative cable velocity is given by Eq. (6a).

A number of researchers (1,2,7) have discussed the forms and magnitudes of the drag components. Their results show that the effects of side and tangential drag on the equilibrium cable shape are negligible compared with the normal drag effects. Consequently, for the purposes of this report, the tangential and side components of drag are set equal to zero. The hydrodynamic force then consists entirely of its normal drag component. If  $v_n$  is used to represent the component of relative velocity which is normal to the cable, the magnitude of the normal drag is known to be  $(1/2) \rho C_D d |v_n|^2$ , where  $d$  is the cable diameter and  $C_D$  is the cable drag coefficient. Since the normal drag acts to resist the normal motion of the cable, its direction of action is given by  $-v_n / |v_n|$ . The hydrodynamic force per unit length  $f_h$  is thus obtained as

$$f_h = -(1/2) \rho C_D d |v_n| v_n . \quad (9a)$$

Further, since the unit tangent to the cable is given by  $d\mathbf{P}/dS$ , the normal and total velocities of the cable are related through the equation

$$v_n = \mathbf{v} - \left( \mathbf{v} \cdot \frac{d\mathbf{P}}{dS} \right) \frac{d\mathbf{P}}{dS} . \quad (9b)$$

which, by using Eq. (6a), becomes

$$v_n = \Omega \mathbf{k} \times \mathbf{P} - \Omega \left[ (\mathbf{k} \times \mathbf{P}) \cdot \frac{d\mathbf{P}}{dS} \right] \frac{d\mathbf{P}}{dS} . \quad (9c)$$

The static equilibrium equation referred to the rotating coordinate system, Eq. 2a, is now developed by setting the external force per unit length  $f$  equal to  $f_w + f_c + f_a + f_h$ . At this point, it is perhaps worthwhile to remark that the equilibrium equations obtained herein can be alternatively obtained from the equations of motion derived by Reid for an arbitrarily towed cable (8) by specializing the equations to an inextensible cable and transforming them to a rotating coordinate system.

#### THE EXTERNAL FORCE ON THE FISH

To complete the specification of the equilibrium problem, the external force of the fish  $F_f$  must be determined. As with the force on the cable, the load on the fish can be divided into gravity and buoyancy forces, centrifugal forces, apparent mass forces, and

hydrodynamic forces. For simplicity of argument, assume that the fish is a nonlifting body and has an axis of symmetry that aligns itself parallel to the flow field.

The weight force on the fish is then given by

$$\mathbf{F}_{fw} = (W - W') \mathbf{k} \quad (10a)$$

where  $W$  is the weight of the fish and  $W'$  is the weight of the displaced fluid. Also, following the same reasoning used in deriving the cable forces, the centrifugal force on the fish becomes

$$\mathbf{F}_{fc} = -M\Omega^2 \mathbf{k} \times (\mathbf{k} \times \mathbf{P}_f) , \quad (10b)$$

where  $M$  is the mass of the fish and  $\mathbf{P}_f$  is its position vector. Similarly, the apparent mass force is given by

$$\mathbf{F}_{fa} = -M'\Omega^2 \mathbf{k} \times (\mathbf{k} \times \mathbf{P}_f) , \quad (10c)$$

where  $M'$  is the appropriate component of the apparent mass tensor of the fish due to its radial acceleration through the fluid.

Because of the nonlifting and symmetry assumptions, the hydrodynamic force on the fish is equal in magnitude to  $(1/2) \rho C_{Df} A_f |\mathbf{V}_f|^2$  and acts in a direction opposed to the velocity of the fish. Consequently, the vector drag force is given by

$$\mathbf{F}_{fh} = -(1/2) \rho C_{Df} A_f |\mathbf{V}_f| \mathbf{V}_f , \quad (10d)$$

where  $C_{Df}$  is the drag coefficient of the fish,  $A_f$  is the appropriate cross-sectional area of the fish, and  $\mathbf{V}_f$  is the velocity of the fish. From Eq. (6a), the velocity of the fish is obtained as

$$\mathbf{V}_f = \Omega \mathbf{k} \times \mathbf{P}_f . \quad (10e)$$

The total external force on the fish  $\mathbf{F}_f$  is now given by  $\mathbf{F}_{fw} + \mathbf{F}_{fc} + \mathbf{F}_{fa} + \mathbf{F}_{fh}$ . Substituting this in the boundary condition at  $S = L$  (Eq. (3b)) and further assuming that  $\mathbf{P}_f = \mathbf{P}(L)$  fully specifies the boundary value-equilibrium problem which determines the shape of a cable towed in a circular path.

## A NONDIMENSIONAL FORM OF THE EQUILIBRIUM EQUATIONS

To determine the important combinations of parameters that appear in the problem, it is necessary to nondimensionalize the equilibrium equations and boundary conditions. This is accomplished by dividing all lengths by the towing radius  $R$  and by dividing the cable tension by  $(\mu + \rho A) gR$ . This quantity is chosen rather than the cable weight in water or the fish weight in water because, in particular cases, either or both of the latter two weights may be zero. With these definitions, the nondimensional arc length  $s$ , the nondimensional position vector  $\mathbf{P}$ , and the nondimensional tension  $T$  become

$$s = S/R , \quad \mathbf{P} = \mathbf{P}/R , \quad T = \tilde{T}/[(\mu + \rho A) gR] .$$

Similarly, the nondimensional coordinates  $x$ ,  $y$ , and  $z$  of the cable point  $s$  are related to the dimensional coordinates by

$$x = X/R , \quad y = Y/R , \quad z = Z/R ,$$

and the nondimensional position vector is given by

$$\mathbf{p} = x\mathbf{i} + y\mathbf{j} + z\mathbf{k} . \quad (11)$$

After substituting these dimensionless quantities into Eq. (2a) and replacing  $f$  by the sum of Eqs. (4), (7), (8), and (9a), the complete static equilibrium equation becomes

$$\frac{d}{ds} \left( T \frac{d\mathbf{p}}{ds} \right) + w\mathbf{k} - \gamma^2 \mathbf{k} \times (\mathbf{k} \times \mathbf{p}) - C\gamma|\gamma| |\mathbf{v}_n^*| \mathbf{v}_n^* = 0 , \quad (12a)$$

where  $\mathbf{v}_n^*$  is the nondimensional normal velocity obtained from Eq. (9c) as

$$\mathbf{v}_n^* = \mathbf{k} \times \mathbf{p} - \left[ (\mathbf{k} \times \mathbf{p}) \cdot \frac{d\mathbf{p}}{ds} \right] \frac{d\mathbf{p}}{ds} . \quad (12b)$$

The nondimensional weight  $w$ , rotational frequency  $\gamma$ , and drag constant  $C$  are defined by

$$w = (\mu - \rho A)/(\mu + \rho A) , \quad (13a)$$

$$\gamma = \Omega \sqrt{R/g} = V/\sqrt{Rg} , \quad (13b)$$

and

$$C = (1/2) \rho C_D dR/(\mu + \rho A) . \quad (13c)$$

Coupled to the equilibrium equations, the geometric constraint, Eq. (2b), becomes

$$\sqrt{\frac{d\mathbf{p}}{ds} \cdot \frac{d\mathbf{p}}{ds}} = 1 . \quad (14)$$

The boundary condition at the towpoint, Eq. (3a), now reads

$$\mathbf{P} \Big|_{s=0} = \mathbf{i} . \quad (15a)$$

On substituting for  $F_f$  the sum of Eqs. (10a, b, c, and d), the boundary condition at the fish, Eq. (3b), becomes in full

$$\left( T \frac{d\mathbf{p}}{ds} \right) \Big|_{s=\lambda} = w_f \mathbf{k} - [m_f \gamma^2 \mathbf{k} \times (\mathbf{k} \times \mathbf{p}) + C_f \gamma |\gamma| |\mathbf{k} \times \mathbf{p}| (\mathbf{k} \times \mathbf{p})] \Big|_{s=\lambda} , \quad (15b)$$

where the nondimensional fish weight  $w_f$ , fish mass  $m_f$ , and fish drag constant  $C_f$  are defined by

$$w_f = (W - W')/[(\mu + \rho A) gR] , \quad (16a)$$

$$m_f = (M + M')/[(\mu + \rho A) R] , \quad (16b)$$

and

$$C_f = (1/2) \rho C_{Df} A_f/(\mu + \rho A) . \quad (16c)$$

The nondimensional cable length  $\lambda$  is defined by

$$\lambda = L/R . \quad (17)$$

Note that  $\lambda$  is the only parameter which contains the actual cable length  $L$ . Consequently, this nondimensionalization of the problem is particularly suited to answering the question: If a ship runs at a speed  $V$  in a circle of radius  $R$ , then what length of cable is needed to place a towed fish at a certain depth below the center of the towing circle?

#### A DISCUSSION OF THE NONDIMENSIONAL PARAMETERS

For the most general case of a cable pulled in a circular path through a dense medium (such as water), seven parameters — four cable parameters  $w$ ,  $\gamma$ ,  $C$ , and  $\lambda$  and three fish parameters  $w_f$ ,  $m_f$ , and  $C_f$  — arise in the equilibrium problem. Actually, this is quite an oversimplification, since the fish has been assumed symmetric and nonlifting and the relation  $\mathbf{p}_f = \mathbf{p}(\lambda)$  has been assumed true. Obviously, the latter assumption must be incorrect, since the fish is a distributed body; and, to obtain the correct boundary conditions at the fish, it is necessary to consider its distributed configuration and the actual point of cable attachment. The complete set of boundary conditions for an arbitrary fish have been derived by Strandhagen and Thomas (9); however, these conditions add only complexity and more parameters to an already complex problem and will be ignored. Even for the simplified boundary conditions given by Eq. (15b), two of the parameters,  $m_f$  (Eq. (16b)) and  $C_f$  (Eq. (16c)), are usually unknown except for very elementary geometric bodies such as spheres, ellipsoids, etc. This is because of lack of knowledge of the quantities  $M'$  and  $C_{Df}$ . Frequently, however, the apparent mass of the fish  $M'$  can be estimated very accurately by analogy with a body of similar shape for which this quantity has been calculated. Several useful examples are contained in Lamb (5).

The drag coefficient  $C_{Df}$  is another case, depending extensively on the shape and alignment of the fish. Fortunately, for solutions of the type desired (the radius of the fish approximately zero), the term containing  $C_f$  in Eq. (15b) can be neglected in comparison with the term containing  $m_f$ . Note first that the vector quantities  $\mathbf{k} \times \mathbf{p}$  and  $\mathbf{k} \times (\mathbf{k} \times \mathbf{p})$  are given by

$$\mathbf{k} \times \mathbf{p} = -y\mathbf{i} + x\mathbf{j}$$

and

$$\mathbf{k} \times (\mathbf{k} \times \mathbf{p}) = -x\mathbf{i} - y\mathbf{j} .$$

Consequently, the centrifugal term in Eq. (15b) is on the order of  $m_f \gamma^2 r_f$ , where  $r_f$  is the radius of the fish, whereas the drag term is on the order of  $C_f \gamma^2 r_f^2$ . The ratio of the drag force to the centrifugal force is then  $C_f r_f / m_f$ , and since it is desired to find solutions such that  $r_f \approx 0$ , this ratio becomes vanishingly small. Thus, with little loss of accuracy, the boundary condition at the fish can be simplified to

$$\left[ T \frac{d\mathbf{p}}{ds} + m_f \gamma^2 \mathbf{k} \times (\mathbf{k} \times \mathbf{p}) \right] \Big|_{s=\lambda} = w_f \mathbf{k} . \quad (18)$$

By eliminating the drag force on the fish, the equilibrium problem in a dense medium has been reduced to one with six known (or easily obtainable) parameters.

In a nondense fluid (such as air), where it is permissible to neglect buoyancy and apparent mass effects, the number of parameters is reduced to four. In such a medium, the cable weight  $w$  (Eq. (13a)) becomes identically equal to unity, and the fish parameters  $w_f$  (Eq. (16a)) and  $m_f$  (Eq. (16b)) become identical, since the weight of the fish  $W$  is equal to  $Mg$ .

In a vacuum ( $\rho=0$ ), only three parameters appear, since the drag constant  $C$  (Eq. (13c)) of the cable vanishes identically.

Furthermore, for the case of a cable to which no fish is attached, the number of parameters for a dense fluid, nondense fluid, and vacuum become, respectively, four, three, and two, since in this case  $w_f$  and  $m_f$  are both zero. These results are summarized in Table 1.

Table 1  
Independent Parameters for Particular Towing Mediums

Medium	Boundary Conditions	Independent Parameters	Special Values
Dense Fluid	With fish	$w, \gamma, C, \lambda$ $w_f, m_f$	For desired solution $C_f = 0$
	Without fish	$w, \gamma, C, \lambda$	$w_f = 0, m_f = 0$
Nondense Fluid	With fish	$\gamma, C, \lambda$ $w_f$	$w = 1$ $m_f = w_f$
	Without fish	$\gamma, C, \lambda$	$w = 1$ $m_f = w_f = 0$
Vacuum	With fish	$\gamma, \lambda$ $w_f$	$w = 1, C = 0$ $m_f = w_f$
	Without fish	$\gamma, \lambda$	$w = 1, C = 0$ $m_f = w_f = 0$

#### RESULTANT FORCE TRANSFORMATION AND THE EQUILIBRIUM EQUATIONS IN COMPONENT FORM

To determine the solution to the set of equilibrium equations, Eqs. (12a) and (14), subject to the boundary conditions, Eqs. (15a) and (18), the equations must first be expressed in their component forms. However, it is obvious that a numerical solution is necessary, and, consequently, it is useful to simultaneously reduce the equilibrium equations to an equivalent set of first-order differential equations. A particularly useful reduction to a set of first-order equations was introduced by Skop and O'Hara (3) and termed the resultant force transformation. To effect this transformation, the resultant force vector  $\mathbf{R}$  is defined by

$$\mathbf{R} = T \frac{d\mathbf{p}}{ds} \quad (19a)$$

or inversely by

$$\frac{d\mathbf{p}}{ds} = \mathbf{R}/T \quad (19b)$$

Substituting Eq. (19b) into the geometric constraint, Eq. (14), the tension  $T$  is expressed in terms of the resultant force through the relation

$$T = \sqrt{\mathbf{R} \cdot \mathbf{R}} \quad (19c)$$

Eqs. (12a) and (19b), coupled with the diagnostic equation, Eq. (19c), form a set of six first-order differential equations for the three components of  $\rho$  and the three components of  $R$ .

Writing

$$R = R_x i + R_y j + R_z k ,$$

substituting for  $\rho$  from Eq. (11), and performing the indicated vector operations in Eq. (12a) result in the equations of equilibrium in component form:

$$\frac{dx}{ds} = R_x/T , \quad (20a)$$

$$\frac{dy}{ds} = R_y/T , \quad (20b)$$

and

$$\frac{dz}{ds} = R_z/T ; \quad (20c)$$

where

$$T = \sqrt{R_x^2 + R_y^2 + R_z^2} . \quad (20d)$$

Also,

$$\frac{dR_x}{ds} + \gamma^2 x + C\gamma|y|\Delta \left[ \left( \frac{xR_y - yR_x}{T} \right) \frac{R_x}{T} + y \right] = 0 , \quad (21a)$$

$$\frac{dR_y}{ds} + \gamma^2 y + C\gamma|y|\Delta \left[ \left( \frac{xR_y - yR_x}{T} \right) \frac{R_y}{T} - x \right] = 0 , \quad (21b)$$

and

$$\frac{dR_z}{ds} + w + C\gamma|y|\Delta \left( \frac{xR_y - yR_x}{T} \right) \frac{R_z}{T} = 0 , \quad (21c)$$

where

$$\Delta = \sqrt{x^2 + y^2 - \left( \frac{xR_y - yR_x}{T} \right)^2} . \quad (21d)$$

To complete the specification of the problem, the end conditions must be written in component form. At  $s = 0$ , Eq. (15a), these become

$$x(0) = 1 , \quad (22a)$$

$$y(0) = 0 , \quad (22b)$$

$$z(0) = 0 , \quad (22c)$$

and at  $s = \lambda$ , Eq. (18), they are

$$R_x(\lambda) - m_f \gamma^2 x(\lambda) = 0 , \quad (23a)$$

$$R_y(\lambda) - m_f \gamma^2 y(\lambda) = 0 , \quad (23b)$$

$$R_z(\lambda) - w_f = 0 . \quad (23c)$$

### SOME EMPIRICAL RESULTS

Even in air, there are four independent parameters (see Table 1) that can have an effect on the equilibrium shape of the cable-fish system. Thus, before attempting an analytical (numerical) solution of the equilibrium equations, it was decided to perform a simple experiment to determine some ranges of parametric values for which the free end of the cable is stationary below the center of the towing circle. The results of this experiment showed several unexpected phenomena which are discussed in this section.

The experimental setup, Fig. 2, consisted of a vertical shaft coupled to a motor driven by a variable autotransformer. A horizontal disk plate, containing a number of holes to be used as cable towpoints, was attached to the end of the shaft. The cable motion was stopped by externally triggered stroboscopes, and photographs of the cable shape were obtained. The frequency of revolution of the vertical shaft was read on a motor-controlled counter.

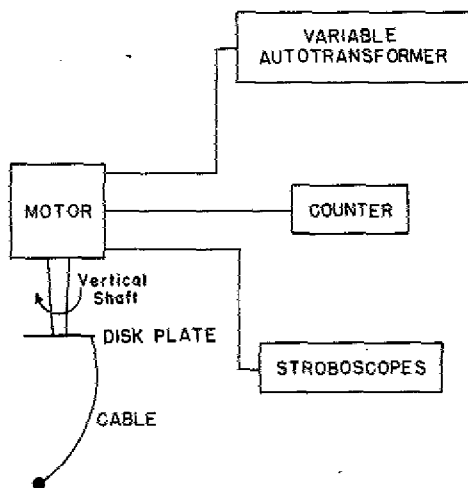


Fig. 2 - Experimental setup

The cable used was a 1/32-in. braided dacron fishing line weighing 0.1824 g/ft. Two different towed bodies, represented by lead fishing sinkers weighing 14.132 g and 16.416 g, were used. The towing medium was air, and to calculate the drag constant  $C$  (Eq. (13c)), a drag coefficient  $C_D$  of 1.2 was assumed. For the results detailed in this report, the towing radius was 11/16 in.

The behavior of the cable system as a function of the independent cable and fish parameters is best discussed and illustrated with reference to some of the pictures which

were obtained. Figs. 3, 4, and 5 show photographs of the cable projection on the  $x-z$  plane together with the values of the parameters  $\gamma$ ,  $\lambda$ ,  $C$ , and  $w_f$  corresponding to the particular figure.

The most important and unusual conclusions to be reached from this experiment concern the nodal point pattern of the cable-fish system. Note that in Fig. 3, the number of nodal points (points where  $x = 0$ ) increases from one to two as  $\gamma$  increases from 1.64 to 5.94. Similarly, in Figs. 4 and 5, the number of nodal points increases from two to three as  $\gamma$  increases from 2.46 to 4.77 and 2.60 to 7.23, respectively. *However, this shift in nodal numbers is not marked by a continuous transition with increasing  $\gamma$ . That is, there are critical values of the rotational frequency  $\gamma$  at which the cable attempts to "jump" from one nodal configuration to the next.* This violent transitional behavior is vividly demonstrated in Fig. 6 where the system corresponding to Fig. 3 ( $\lambda = 37.8$ ,  $C = 0.018$ ,  $w_f = 1352$ ) is attempting to jump from its one-node to its two-node configuration at  $\gamma \approx 3.9$ .

Several other physical phenomena which must be predicted by the equilibrium equations are readily discernible from Figs. 3 to 5. To place these in an appropriate mathematical form, let  $\gamma_{cn}(\lambda, C, w_f)$  represent that value of  $\gamma$  for which a fixed system ( $\lambda$ ,  $C$ , and  $w_f$  constant) jumps from its  $(n-1)$ st to its  $n$ th nodal configuration. Also, let  $R_{x0}$  be the value of the  $x$  component of the resultant force at  $s = 0$  (the attachment point of the ship and the cable), and let  $R_{x0}^{cn}(\lambda, C, w_f)$  be the value of  $R_{x0}$  immediately following transition to the  $n$ th nodal shape. Then, with reference to Figs. 3, 4, and 5, the following conclusions can be drawn from the present experiment:

1. For fixed  $C$  and  $w_f$ , the critical values of  $\gamma$  decrease as  $\lambda$  increases. (Fig. 3b, one node at  $\gamma = 2.97$  vs Fig. 4a, two nodes at  $\gamma = 2.46$ ; and Fig. 3c, two nodes at  $\gamma = 5.94$  vs Fig. 4c, three nodes at  $\gamma = 4.77$ .) This result can be expressed mathematically as

$$\gamma_{cn}(\lambda_1, C, w_f) < \gamma_{cn}(\lambda_2, C, w_f) , \quad (24a)$$

if

$$\lambda_1 > \lambda_2 . \quad (24b)$$

2. For fixed  $C$  and  $\lambda$ , the critical values of  $\gamma$  decrease as  $w_f$  decreases. (Fig. 4c, three nodes at  $\gamma = 4.77$  vs Fig. 5b, two nodes at  $\gamma = 4.77$ .) Mathematically, this result can be summarized as

$$\gamma_{cn}(\lambda, C, w_{f1}) < \gamma_{cn}(\lambda, C, w_{f2}) , \quad (25a)$$

if

$$w_{f1} < w_{f2} . \quad (25b)$$

3. Immediately following transition  $dx/ds$  is negative at  $s = 0$  (Figs. 3a, 4a, 4c, and 5a). Since, from Eq. (20a), the sign of  $dx/ds$  is the same as the sign of  $R_x$ , this result gives

$$R_{x0}^{cn}(\lambda, C, w_f) < 0 . \quad (26a)$$

As  $\gamma$  increases,  $dx/ds$  at  $s = 0$  becomes continuously more positive until the next transition point is reached. (Compare Figs. 3a and 3b, Figs. 4a and 4b, and Figs. 5a and 5b.) Again using Eq. (20a), this means that

$$\frac{dR_{x0}}{d\gamma} > 0 \quad (26b)$$

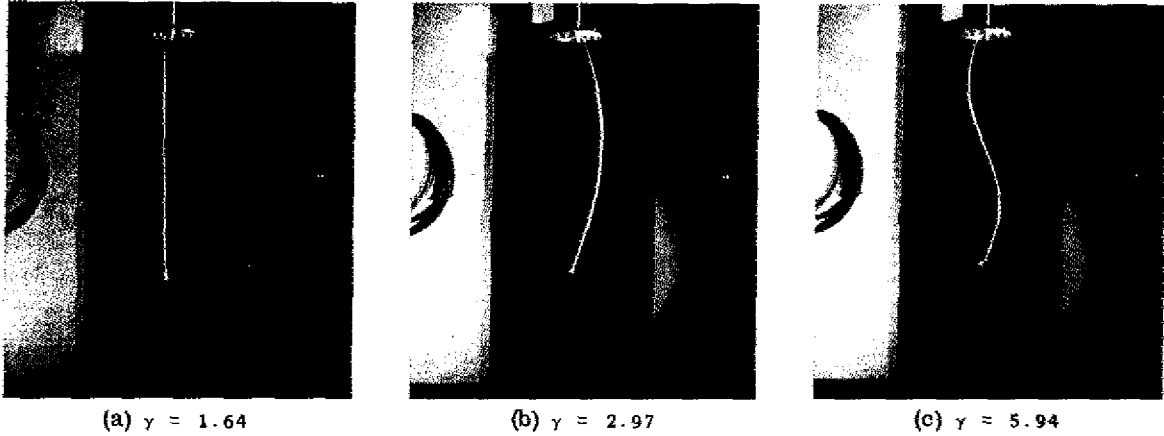


Fig. 3 - Experimental  $x-z$  projections for the circularly towed cable system  
 $\lambda = 37.8$ ,  $C = 0.018$ ,  $w_f = 1352$

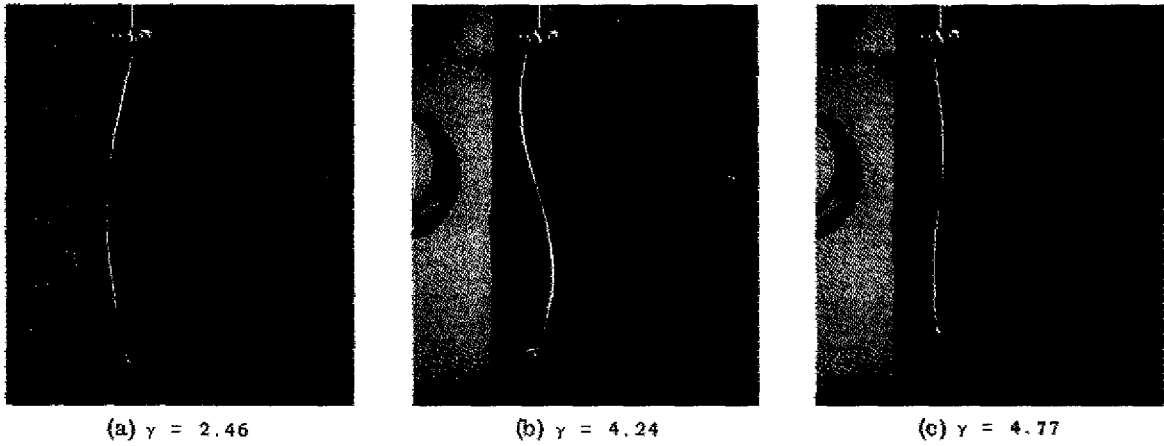


Fig. 4 - Experimental  $x-z$  projections for the circularly towed cable system  
 $\lambda = 52.4$ ,  $C = 0.018$ ,  $w_f = 1352$

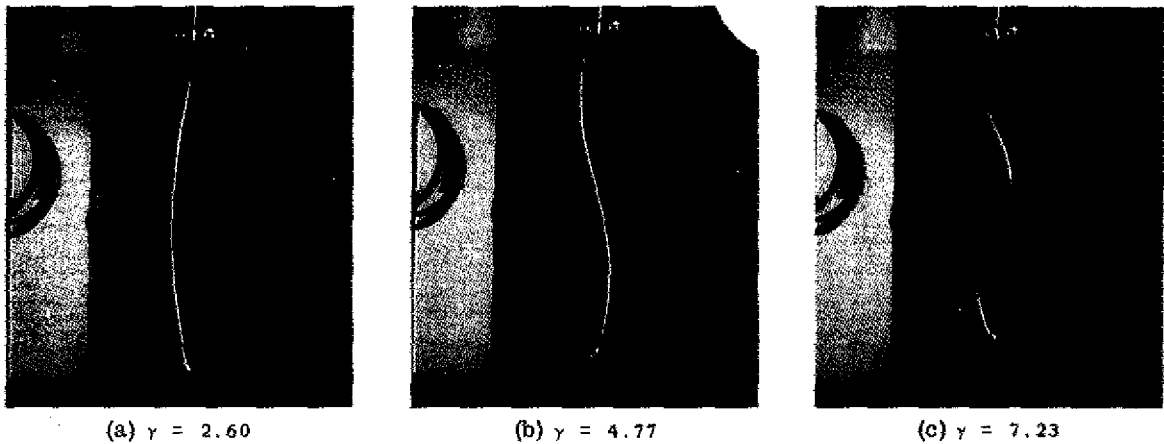


Fig. 5 - Experimental  $x-z$  projections for the circularly towed cable system  
 $\lambda = 52.4$ ,  $C = 0.018$ ,  $w_f = 1571$

Fig. 6 - One- to two-node transitional behavior at  $\gamma \approx 3.9$  for the circularly towed cable system  $\lambda = 37.8$ ,  $C = 0.018$ ,  $w_f = 1352$



for

$$\gamma_{c(n-1)}(\lambda, C, w_f) < \gamma < \gamma_{cn}(\lambda, C, w_f) . \quad (26c)$$

No conclusions can be drawn from this experiment concerning the effects of the drag constant  $C$  on the critical values of  $\gamma$ . In fact, for most of the cases discussed in this section, the effect of drag on the equilibrium cable shape is negligible as shown in the  $y-z$  planar projections of Figs. 7 and 8. (As will be shown later, the influence of drag can be surmised by the amount of deflection of the cable away from  $y = 0$ .) The  $y-z$  projection of Fig. 7a corresponds to the  $x-z$  projection of Fig. 3a, and similarly for Figs. 7b and 3b, 7c and 3c, 8a and 4a, and 8b and 4c. It is seen that only in the latter case has the influence of drag become significant in determining the equilibrium shape.

#### ON THE SHAPE IN A VACUUM

The equations of static equilibrium cannot, of course, be used to study the complex dynamic transitional behavior of the cable. This does not, however, negate their validity for predicting the onset of unstable behavior and for determining the cable shape when static solutions are possible. To ascertain whether the theoretical equations do indeed possess these properties and the additional properties described by Eqs. (24) to (26), it is useful to make all of the rational simplifications which are possible.

Since the experimental results detailed in the last section indicated small deflections of the cable away from  $y = 0$  (Figs. 7 and 8), the most natural theoretical simplification is to assume that

$$y = 0 . \quad (27a)$$

Substituting Eq. (27a) into Eq. (20b), then, gives

$$R_y = 0 . \quad (27b)$$

The null results given by Eqs. (27a and b) identically satisfy the  $y$ -directional boundary conditions at the ship and fish, Eqs. (22b) and (23b), respectively. However, these results do not satisfy the equation of equilibrium in the  $y$  direction, Eq. (21b), unless the drag constant  $C = 0$ . This means, of course, that the assumption  $y = 0$  is equivalent to assuming a vacuous towing medium (see Table 1). Since the experimental value of  $C$  was 0.018, the assumption of a vacuous medium for a preliminary study of the equations of equilibrium seems justified. Note that this assumption, while greatly simplifying the

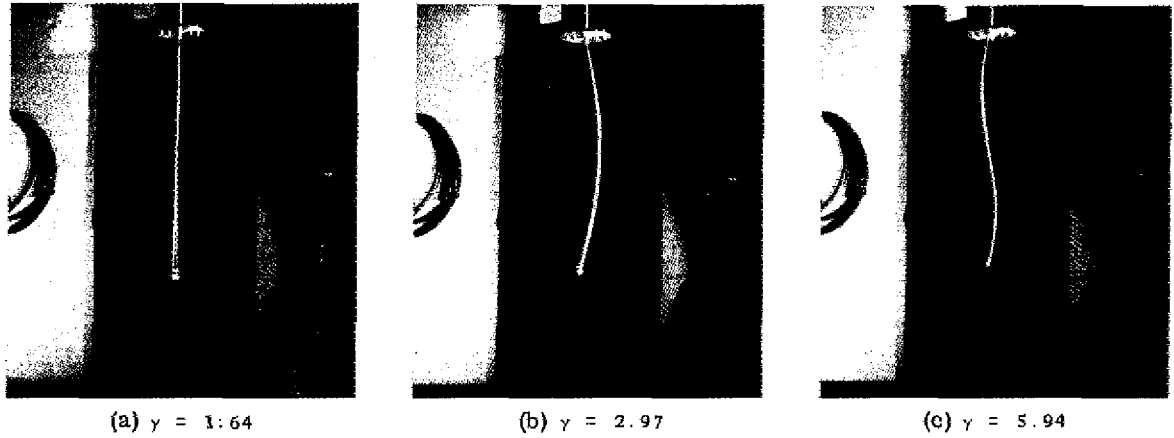


Fig. 7 - Experimental  $y$ - $z$  projections for the circularly towed cable system  
 $\lambda = 37.8, C = 0.018, w_f = 1352$

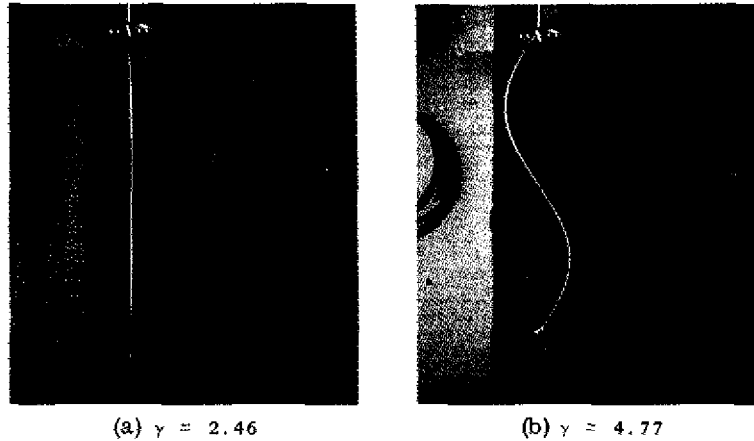


Fig. 8 - Experimental  $y$ - $z$  projections for the circularly towed cable system  $\lambda = 52.4, C = 0.018, w_f = 1352$

equilibrium equations, retains the basic characteristic which distinguishes towing in a circle from towing in a straight line. This is the presence of a centrifugal force acting on the cable.

The equilibrium equation in the  $z$  direction (Eq. (21c)), when specified to a vacuum ( $C = 0, w = 1$ ), becomes

$$\frac{dR_z}{ds} + 1 = 0 .$$

The integral of this equation which satisfies the  $z$ -directional boundary condition at the fish, Eq. (23c), is given by

$$R_z = w_f + (\lambda - s) . \quad (28)$$

By substituting the values of  $R_y$  (Eq. (27b)) and  $R_z$  (Eq. (28)) into Eq. (20d) for the tension  $T$ , the solution for the shape of a cable towed in a circular path through a vacuum can be reduced to integrating two first-order differential equations for  $x$  and  $R_x$  obtained from Eqs. (20a) and (21a), as

$$\frac{dx}{ds} = \frac{R_x}{\sqrt{[w_f + (\lambda - s)]^2 + R_x^2}} \quad (29a)$$

and

$$\frac{dR_x}{ds} = -\gamma^2 x \quad (29b)$$

At  $s = 0$ , the solution of these equations must satisfy the boundary condition given by Eq. (22a); and since in a vacuum  $m_f = w_f$ , the boundary condition at  $s = \lambda$  is derived from Eq. (23a) as

$$R_x(\lambda) - w_f \gamma^2 x(\lambda) = 0 \quad (30)$$

Once the solution for  $R_x$  has been obtained, the solution for  $z$  which satisfies the boundary condition Eq. (22c) can be found from the integral of Eq. (20c) as

$$z = \int_0^s \frac{w_f + (\lambda - \xi)}{\sqrt{[w_f + (\lambda - \xi)]^2 + R_x^2}} d\xi \quad (31)$$

#### METHOD OF SOLUTION

The formal integral of Eq. (29a) which satisfies the boundary condition  $x(0) = 1$  (Eq. (22a)) is given by

$$x = 1 + \int_0^s \frac{R_x}{\sqrt{[w_f + (\lambda - \xi)]^2 + R_x^2}} d\xi \quad (32a)$$

Similarly, the formal integral of Eq. (29b) can be written as

$$R_x = R_{x0} - \gamma^2 \int_0^s x d\xi \quad (32b)$$

where now, however,  $R_{x0}$  is a constant of integration which must be chosen so that the boundary condition at  $s = \lambda$ , Eq. (30), is satisfied.

(Note that once some value of  $R_{x0}$  has been assumed, the values of  $x(\lambda)$  and  $R_x(\lambda)$  can be obtained by a numerical integration of Eqs. (32a) and (32b). In this report, the fourth-order Runge-Kutta method (see Ref. 10) has been used to perform the integrations, and all calculations have been done with the cable length divided into 100 segments.)

In general, for an arbitrary guess at  $R_{x0}$ , the boundary condition at  $s = \lambda$  is not satisfied. If the error at  $\lambda$ ,  $E(\lambda)$ , due to this guess is defined by

$$E(\lambda) = R_x(\lambda) - w_f \gamma^2 x(\lambda) \quad (33)$$

the method of solution then consists of making repeated guesses at  $R_{x_0}$  until a value (or values) is found for which  $E(\lambda) = 0$ . Since this is a hit-or-miss method, it is desirable, if possible, to bound the values which  $R_{x_0}$  may take so that the search can be localized. This is easily accomplished.

Consider first  $x$ . Since the integrand in Eq. (32a) is bounded between  $\pm 1$ , the value of  $x(s)$  can be bounded as

$$1 - s < x(s) < 1 + s .$$

Now consider the boundary condition Eq. (30). Using Eqs. (32b) and (33), this condition can be rewritten as

$$E(\lambda) = R_{x_0} - w_f \gamma^2 x(\lambda) - \gamma^2 \int_0^\lambda x \, ds = 0 . \quad (34)$$

Using the lower and upper bounds of  $x(s)$ , the term

$$w_f \gamma^2 x(\lambda) + \gamma^2 \int_0^\lambda x \, ds$$

can be limited to the range

$$w_f \gamma^2 (1 - \lambda) + \gamma^2 \int_0^\lambda (1 - s) \, ds < w_f \gamma^2 x(\lambda) + \gamma^2 \int_0^\lambda x \, ds < w_f \gamma^2 (1 + \lambda) + \gamma^2 \int_0^\lambda (1 + s) \, ds .$$

In this inequality, the left-hand side (l.h.s.) gives the minimum value which *must* be subtracted from  $R_{x_0}$ , and the right-hand side (r.h.s.) gives the maximum value which *can* be subtracted from  $R_{x_0}$ . Consequently, from Eq. (34),  $E(\lambda)$  must be negative if  $R_{x_0}$  is less than the left-hand side of the inequality. Similarly,  $E(\lambda)$  must be positive if  $R_{x_0}$  is greater than the right-hand side of the inequality. Thus, the range of values of  $R_{x_0}$  for which  $E(\lambda)$  can possibly equal zero is bounded to

$$l. h. s. < R_{x_0} < r. h. s.$$

Evaluating the integrals which appear in the inequality, this condition can be expressed analytically as

$$-\gamma^2 \left[ \frac{\lambda^2}{2} + \lambda(w_f - 1) - w_f \right] < R_{x_0} < \gamma^2 \left[ \frac{\lambda^2}{2} + \lambda(w_f + 1) + w_f \right] . \quad (35)$$

All possible solutions of Eqs. (32a and b), subject to the boundary condition Eq. (34), can now be found by obtaining a plot of  $E(\lambda)$  vs  $R_{x_0}$  over the range of values of  $R_{x_0}$  given by Eq. (35). Such a curve is called a "solution curve"; and, as stated previously, those values of  $R_{x_0}$  for which  $E(\lambda) = 0$  are consistent solutions of the boundary value problem. Note that, within this range for  $R_{x_0}$ , there exists at least one consistent solution. This follows from the fact that  $E(\lambda)$  changes from negative to positive as  $R_{x_0}$  proceeds from the left-hand to the right-hand side of the range.

THE CHARACTER OF THE SOLUTIONS FOR  $\lambda \leq \lambda_c$   
(ZERO-NODE SOLUTIONS)

It is geometrically obvious that no equilibrium cable shape containing a nodal point can exist if  $\lambda < 1$ . However, it does not necessarily follow that a nodal equilibrium solution can be obtained if  $\lambda > 1$ . Thus, the condition that  $\lambda > 1$  is a necessary, but not sufficient, condition for the existence of nodal solutions. In this section, a best value of  $\lambda$ ,  $\lambda_c$ , is determined such that for  $\lambda \leq \lambda_c$  no nodal solutions are possible. Conversely, since this is a best value, it must follow that nodal solutions can exist if  $\lambda > \lambda_c$ . That this is true will be shown in the next section of the report.

Recall the experimental result that  $R_{x_0}$  is negative immediately following transition to a higher order nodal solution, Eq. (26a), and let it be postulated that the best condition for the nonexistence of nodal solutions can be obtained by limiting the possible equilibrium values of  $R_{x_0}$  to a positive range. According to Eq. (35), this situation can occur only if the left-hand side of the inequality bounding  $R_{x_0}$  is positive. The postulate then assumes the form that nodal solutions cannot exist if  $\lambda \leq \lambda_c$ , where  $\lambda_c$  is the solution of

$$\frac{\lambda_c^2}{2} + \lambda_c(w_f - 1) - w_f = 0 .$$

The physically acceptable solution of this equation (positive  $\lambda_c$ ) is

$$\lambda_c = 1 - w_f + \sqrt{1 + w_f^2} . \quad (36)$$

The curve of  $\lambda_c$  vs  $w_f$  is plotted in Fig. 9. Note that  $\lambda_c$  is always greater than unity.

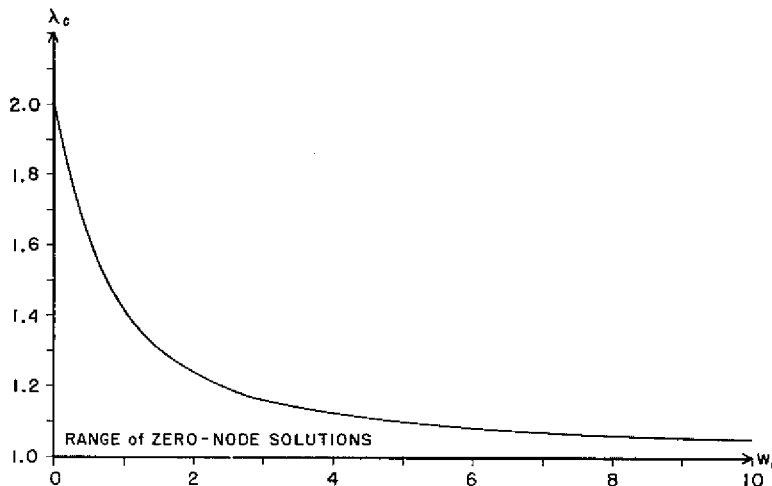


Fig. 9 - The critical value of  $\lambda$ ,  $\lambda_c$ , vs  $w_f$

The proof of this postulate is, unfortunately, numerical rather than analytical and consists of obtaining solution curves for the triplet  $(w_f, \lambda \leq \lambda_c, \gamma)$  over a wide range of values. In particular, solution curves have been obtained for all possible combinations of

$$w_f = 0, 10, 20, \dots, 100,$$

$$\lambda = \lambda_c, \lambda_c - 0.01, \lambda_c - 0.02, \dots, 1,$$

and

$$\gamma = 1, 19, 29, 39, \dots, 99.$$

By using these solution curves, the equilibrium values of  $R_{x_0}$  have been found and the corresponding equilibrium cable shapes determined.

The general shape of the solution curves obtained in these calculations is shown in Fig. 10. In particular, curve (a) corresponds to  $w_f = 0$ ,  $\lambda = \lambda_c = 2$ , and  $\gamma = 39$ ; and curve (b) to  $w_f = 10$ ,  $\lambda = \lambda_c = 1.05$ , and  $\gamma = 19$ . The curves for all other values of  $w_f$ ,  $\lambda = \lambda_c$ , and  $\gamma$  are similar, as are the solution curves for  $\lambda < \lambda_c$ . For the latter curves, of course, the left-hand side of the possible range for  $R_{x_0}$  is greater than zero. A typical example is shown in curve (c) for  $w_f = 0$ ,  $\lambda = 1.8$ , and  $\gamma = 39$ .

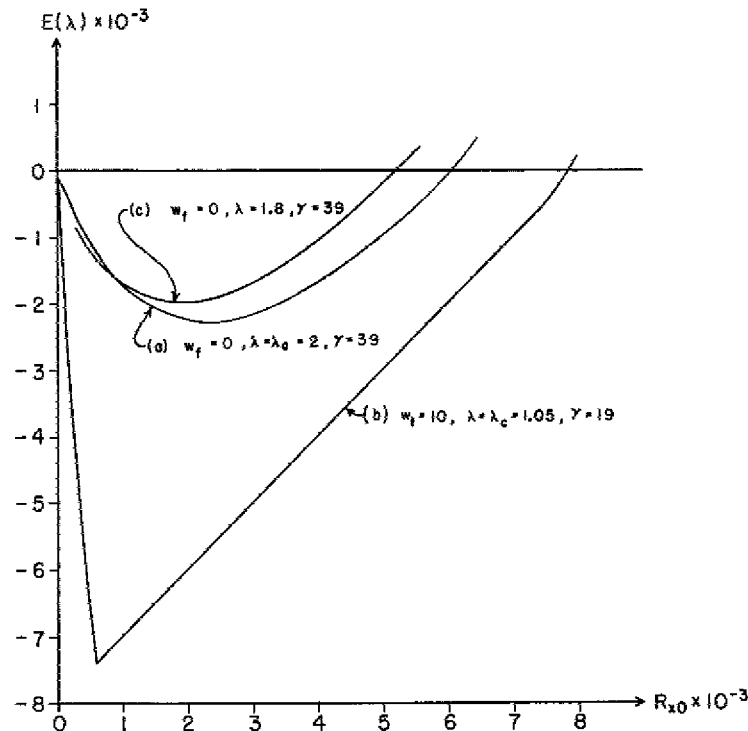
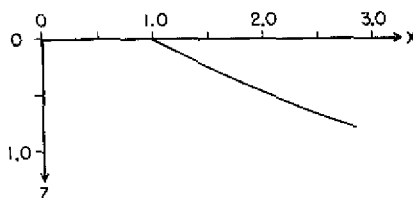


Fig. 10 - Typical solution curves for  $\lambda \leq \lambda_c$

The most important thing to notice about these solution curves is that for each curve there exists only one value of  $R_{x_0}$  for which  $E(\lambda) = 0$ . That is, for  $\lambda \leq \lambda_c$ , there is only one possible equilibrium cable shape. In Fig. 11, a typical equilibrium configuration generated by this solution is shown. For this particular example,  $w_f = 0$ ,  $\lambda = \lambda_c = 2$ , and  $\gamma = 1$ . The equilibrium value of  $R_{x_0}$  is given by 3.79886. Note that in this configuration the  $x$  coordinate of the cable is monotonically increasing from  $x = 1$ . Obviously, such a shape corresponds to a non-nodal solution, thereby verifying the postulate that nodal equilibrium configurations cannot exist if  $\lambda \leq \lambda_c$ .

Fig. 11 - Typical zero-node cable shape for  $\lambda \leq \lambda_c$ ; in particular,  $w_f = 0$ ,  $\lambda = \lambda_c = 2$ ,  $\gamma = 1$



#### THE CHARACTER OF THE SOLUTIONS FOR $\lambda > \lambda_c$ (NODAL SOLUTIONS)

To examine the behavior of the solutions for  $\lambda > \lambda_c$ , a series of solution curves have been determined for the triplet  $(w_f, \lambda = \lambda_c + 0.1, \gamma)$ . The values of  $w_f$  again range from 0 to 100 in steps of 10, and the curves have been calculated at various values of  $\gamma$ . The character of these solution curves is drastically different from the curves obtained for  $\lambda \leq \lambda_c$ . A typical series of curves is shown in Fig. 12 for  $w_f = 0$ ,  $\lambda = 2.1$ , and  $\gamma = 3.8, 5.0$ , and  $6.2$ .

Note that for  $\gamma = 3.8$  and  $5.0$ , only one value of  $R_{x_0}$ , denoted by  $R_{x_0}^a$ , exists for which the boundary condition  $E(\lambda) = 0$  is satisfied. The cable shape corresponding to this solution is similar to the shape depicted in Fig. 11; that is, the cable swings outward from  $x = 1$ . However, as  $\gamma$  increases to  $6.2$ , three solutions which satisfy the boundary condition becomes possible. These are denoted by  $R_{x_0}^a$ ,  $R_{x_0}^{br}$ , and  $R_{x_0}^{bl}$ . The cable shape corresponding to the solution  $R_{x_0}^a$  is again similar to Fig. 11. The shapes corresponding to  $R_{x_0}^{br}$  and  $R_{x_0}^{bl}$  are shown in Fig. 13. Note that the latter equilibrium configurations each contain one nodal point.

For all of the cases studied with  $\lambda = \lambda_c + 0.1$ , this three-solution behavior (with the corresponding zero- and one-node cable shapes) initiates at  $\gamma < 20$  and persists to  $\gamma = 100$ , which is the largest value of  $\gamma$  used for calculating the solution curves. Thus, these results indicate that for  $\lambda = \lambda_c + 0.1$  no solutions exist which can generate cable shapes having more than one nodal point.

As  $\lambda$  becomes increasingly greater than  $\lambda_c$ , the nature of the solution curves becomes increasingly more complex and interesting. Fig. 14 details a series of these curves for  $w_f = 0$  and  $\lambda = 10$  at values of  $\gamma$  equal to  $0.5, 1.0$ , and  $1.5$ . Note that for  $\gamma = 0.5$ , there are three possible solutions of the equilibrium problem. As before, these are denoted by  $R_{x_0}^a$ ,  $R_{x_0}^{br}$ , and  $R_{x_0}^{bl}$ , and generate, respectively, zero-node, one-node, and one-node cable shapes. As  $\gamma$  increases to  $1.0$ , the number of solutions (and corresponding shapes) remains the same. However, the solution  $R_{x_0}^{bl}$  has become more negative while the solution  $R_{x_0}^{br}$  has become more positive. Finally, as  $\gamma$  increases to  $1.5$ , five solutions become possible. These two additional solutions are denoted by  $R_{x_0}^{dr}$  and  $R_{x_0}^{dl}$  and generate the two-node equilibrium shapes shown in Fig. 15.

Note that these two additional solutions fall between  $R_{x_0}^{br}$  and  $R_{x_0}^{bl}$ . As has been demonstrated by other calculations not reproduced in this report, this is a typical and consistent behavior of the solutions curves. In other words, *additional possible equilibrium solutions always arise in pairs, and these two additional solutions are always the first two solutions directly to the left of the previous median solution*. Thus, in Fig. 14, when  $\gamma = 1.5$ ,  $R_{x_0}^{dr}$  and  $R_{x_0}^{dl}$  are the first two solutions to the left of  $R_{x_0}^{br}$  which is the median solution when  $\gamma = 1.0$ . Similarly, in Fig. 12, when  $\gamma = 6.2$ ,  $R_{x_0}^{br}$  and  $R_{x_0}^{bl}$  are the first two solutions to the left of  $R_{x_0}^a$  which is the median (and only) solution when  $\gamma = 5.0$ . This behavior, coupled with the fact that  $E(\lambda)$  changes from negative to positive as  $R_{x_0}$  proceeds from the left-hand to the right-hand side of its possible range of values (Eq.

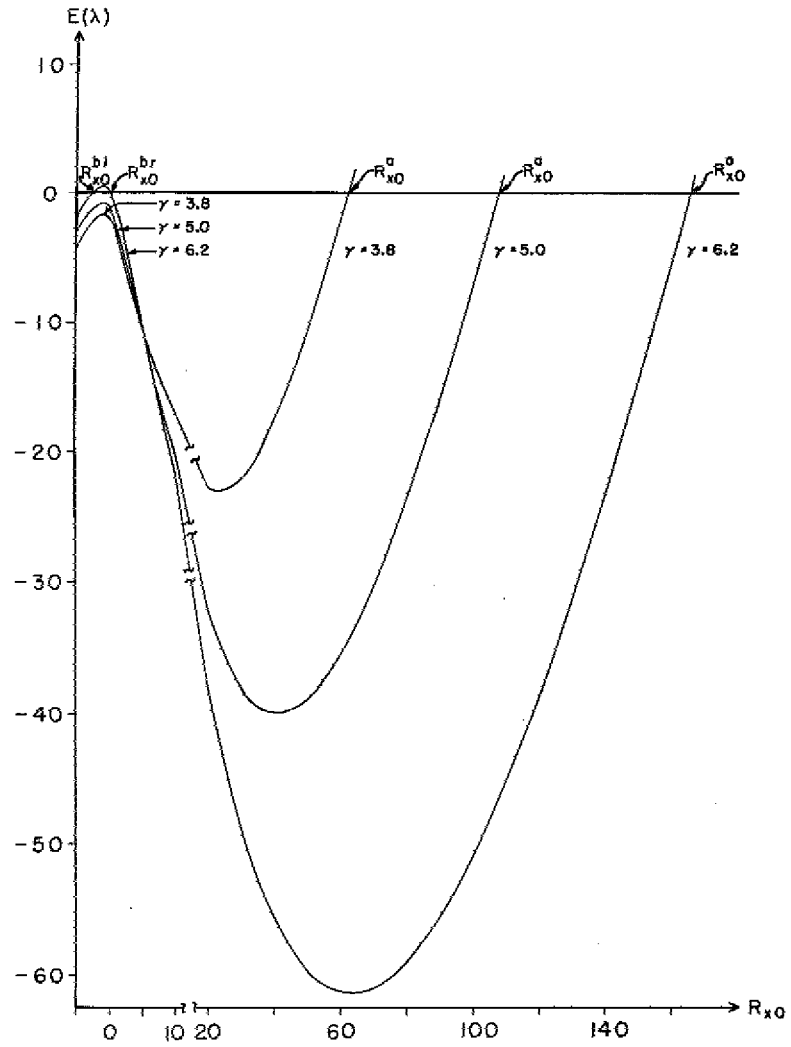


Fig. 12 - A series of solution curves for  $\lambda = 2.1$ ,  $w_f = 0$

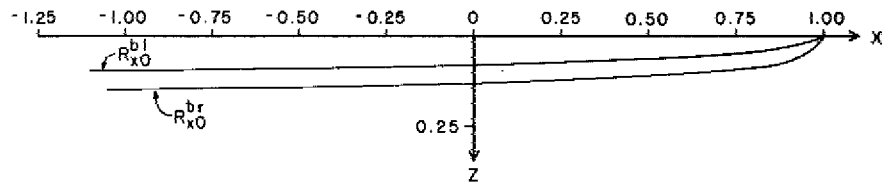


Fig. 13 - One-node cable shapes generated by the equilibrium values  $R_{x0}^{br}$  and  $R_{x0}^{bl}$  for  $\lambda = 2.1$ ,  $w_f = 0$ ,  $\gamma = 6.2$

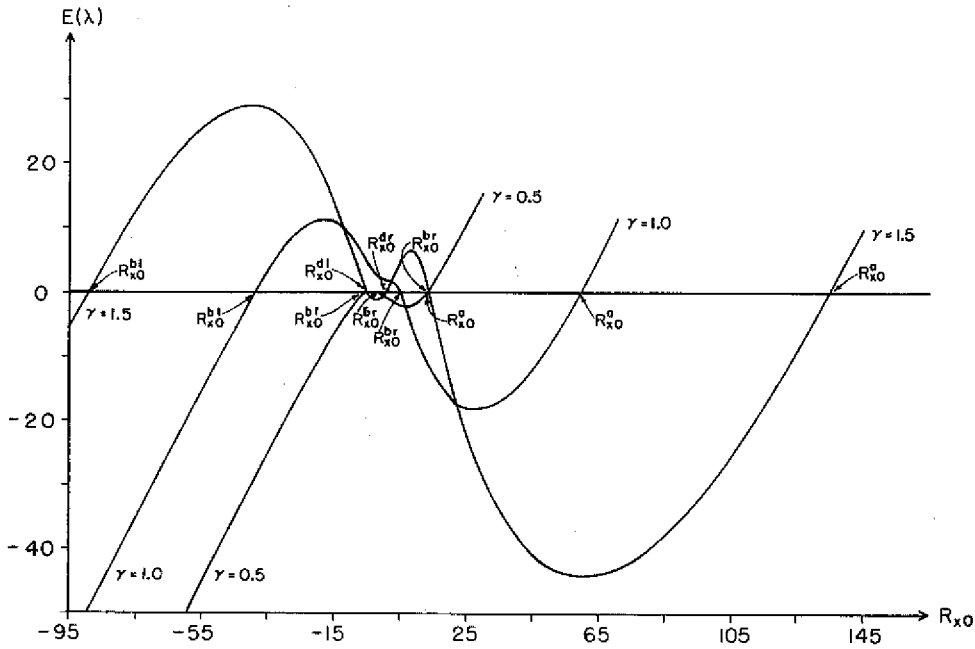


Fig. 14 - A series of solution curves for  $\lambda = 10, w_f = 0$

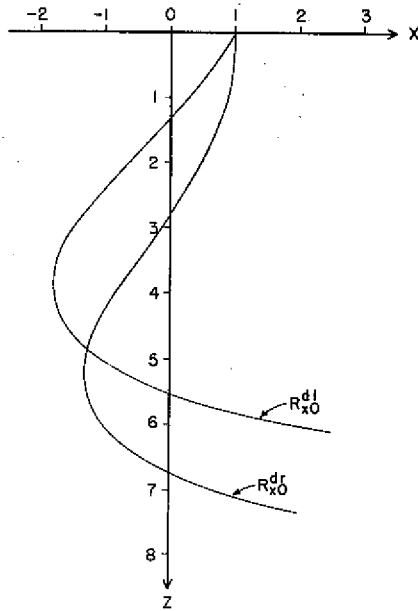


Fig. 15 - Two-node cable shapes generated by the equilibrium values  $R_{x0}^{dr}$  and  $R_{x0}^{dl}$  for  $\lambda = 10, w_f = 0, \gamma = 1.5$

(35)), is sufficient to guarantee that each solution curve can have only an odd number of roots, one of which may be a double (tangent) root. Note, for example, that in Fig. 14 the solution curve for  $\gamma = 0.5$  has just passed the condition of tangency.

Since for  $\lambda > \lambda_c$  it is possible to generate more than one equilibrium solution, a small perturbation dynamic analysis about each solution would be necessary to analytically determine which of the cable shapes are stable and which are unstable. This treatment is quite complex, especially since the equilibrium configurations are known only numerically. Fortunately, in lieu of a small perturbation analysis, the experimental results can be used to develop an interpretation of the solution curves.

In the experimental results for fixed  $\lambda$  and  $w_f$ , recall that the number of nodes increases as  $\gamma$  increases, that immediately following transition the value of  $R_{x_0}$  is negative (Eq. (26a)), and that between transitions the equilibrium value of  $R_{x_0}$  becomes continuously more positive with increasing  $\gamma$  (Eqs. (26b and c)). The following interpretation of the solution curves is then logical and consistent. For fixed  $\lambda$  and  $w_f$ , then,

1. For small  $\gamma$ , only one solution, the zero-node solution, is possible.
2. As  $\gamma$  increases, and for  $\lambda > \lambda_c$ , a double root is approached. This root is always to the left of the previous median (and only) solution. The value of  $\gamma$  for which the double root occurs represents a transitional instability. In fact, this value of  $\gamma$  is  $\gamma_{c1}(\lambda, w_f)$  since the double root generates a one-node equilibrium configuration.
3. As  $\gamma$  increases further, the median root ( $R_{x_0}^{br}$  in Figs. 12 and 14) determines the stable configuration.
4. As  $\gamma$  increases still further, the solution curve again approaches a tangency condition if  $\lambda$  is sufficiently large. (Recall that for  $\lambda = \lambda_c + 0.1$  this second tangency condition does not appear.) This double root always occurs between the previous median solution and the solution directly to the left of the previous median solution. The value of  $\gamma$  for which this double root occurs is  $\gamma_{c2}(\lambda, w_f)$ , since this root marks the transition from a one-node to a two-node solution.
5. As  $\gamma$  increases from  $\gamma_{c2}(\lambda, w_f)$ , the new median solution ( $R_{x_0}^{dr}$  in Fig. 14) determines the stable configuration.
6. For sufficiently large  $\lambda$ , steps 4 and 5 are a continually repeating process.

To demonstrate the validity of this interpretation, the problem of predicting the cable shapes shown in Fig. 3 is considered. The calculations are, of course, idealized to a vacuum medium. For the set of photographs in Fig. 3, the dimensionless cable length  $\lambda$  is equal to 37.8 and the dimensionless fish weight  $w_f$  is given by 1352. Figs. 3a, b, and c correspond, respectively, to rotational frequencies  $\gamma$  of 1.64, 2.97, and 5.94.

The solution curves for this problem are plotted in Fig. 16, and the value of the median root obtained for each  $\gamma$  is

$$\text{for } \gamma = 1.64, \quad R_{x_0} = 5.543629;$$

$$\text{for } \gamma = 2.97, \quad R_{x_0} = 552.265381;$$

and

$$\text{for } \gamma = 5.94, \quad R_{x_0} = 534.242818.$$

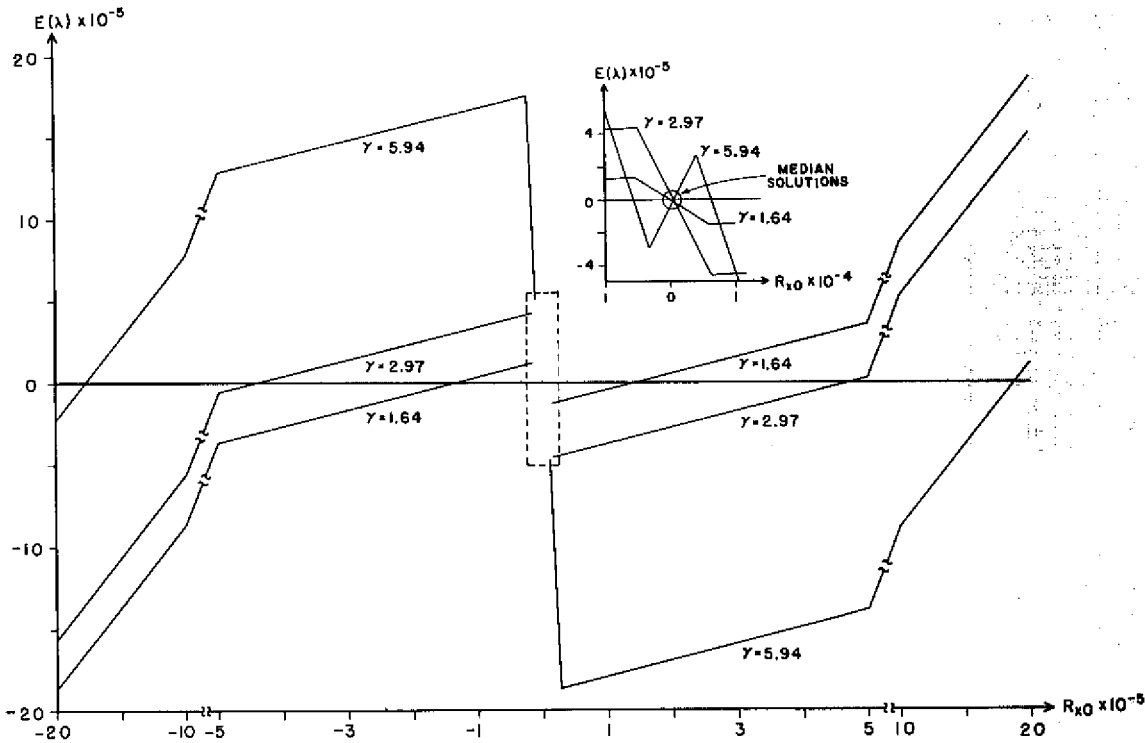


Fig. 16 - Solution curves for  $\lambda = 37.8, w_f = 1352$

These roots have been calculated to an accuracy of  $|E(\lambda)| < 10^{-5}$ . The cable shapes generated by the median solutions are shown in Fig. 17. The marked similarity between the theoretical shapes in Fig. 17 and the experimental photographs of Fig. 3 is obvious and verifies the above interpretation of the solution curves.

**SOME QUALITATIVE CONSIDERATIONS**

In order to construct a table showing perhaps  $x(\lambda)$  and  $z(\lambda)$  vs  $\gamma, \lambda$ , and  $w_f$ , it would first be necessary to construct an auxiliary table which would give the critical values of  $\gamma, \gamma_{cn}(\lambda, w_f)$ , and the corresponding critical values of  $R_{x0}, R_{x0}^{cn}(\lambda, w_f)$ , since these values mark transitional points of the stable solution. This represents a massive computational problem and will not be pursued here. However, certain qualitative remarks concerning the auxiliary table can be made.

First, to be in accord with the experimental results, the table should show that for fixed  $w_f$  the critical values of  $\gamma$  decrease as  $\lambda$  increases (Eqs. (24a and b)). That the theoretical calculations do predict this behavior may be seen by referring to Figs. 12 and 14. From Fig. 12, it is seen that  $\gamma_{c1}(2.1, 0) \approx 6.2$ , whereas from Fig. 14,  $\gamma_{c1}(10., 0) \approx 0.5$ . Also, from previous discussions,  $\gamma_{c2}(2.1, 0)$ , if it exists, is greater than 100; while, again from Fig. 14,  $\gamma_{c2}(10., 0) \approx 1.5$ .

The second experimental conclusion (Eqs. (25a and b)) that

$$\gamma_{cn}(\lambda, w_{f1}) < \gamma_{cn}(\lambda, w_{f2}) \text{ if } w_{f1} < w_{f2}$$

is not always true. That this is so can be readily shown. Suppose  $\lambda = 2$  and  $w_{f1} = 0$  while  $w_{f2} = 100$ . Then for  $w_{f1}$ ,  $\lambda = \lambda_c$  and no critical rotational speed exists; whereas for  $w_{f2}$ ,  $\lambda > \lambda_c$  and thus a critical finite rotational speed does exist. On the other hand, as  $\lambda$  increases, this character may change. Thus, from Fig. 14,  $\gamma_{c2}(10., 0) \approx 1.5$ . Consequently, from Eqs. (24a and b),  $\gamma_{c2}(37.8, 0) < 1.5$ . Meanwhile, from Fig. 16, it is seen that  $\gamma_{c2}(37.8, 1352) > 2.97$ . Thus

$$\gamma_{c2}(37.8, 0) < \gamma_{c2}(37.8, 1352) ,$$

in accordance with the experimental observations.

## CONCLUSIONS

This report has considered, both by experimental and theoretical means, the quasi-static problem of determining the shape of a cable towed in a circular path. For the present, these studies have been restricted to cases where the effect of hydrodynamic drag is negligible.

The results of the experimental approach show many surprising phenomena, of which the most important is that for certain combinations of the governing parameters no stable equilibrium solution for the cable shape exists. Rather, at these combinations of parameters, the system is marked by a violent dynamic motion between two adjoining nodal configurations.

To study this phenomenon theoretically, the static equilibrium equations have been idealized to a vacuum medium. It has been shown that the solution to these equations is not unique. That is, for a given set of parameters, several equilibrium configurations are possible. The questions of stability of equilibrium and onset of transition have been resolved from these solutions by reference to the experimental observations.

Unfortunately, the results in this report have been obtained by necessity from extensive numerical calculations. This leaves as rather undefined the essential physical and analytical reasons for the behavior of the cable-fish system. Noteworthy as missing is a theoretical stability analysis of the possible equilibrium shapes. However, since no drag forces are present in a vacuum, it can be concluded that the centrifugal force on the cable is the principal agent responsible for producing the unsteady transitional behavior.

The extension of the methods and arguments in this report to the more realistic problem with drag included is by no means trivial. When drag is introduced into the equilibrium equations (Eqs. (21a, b, and c)), there are three, rather than one, unknown reaction components at the towpoint. Consequently, the calculation and interpretation

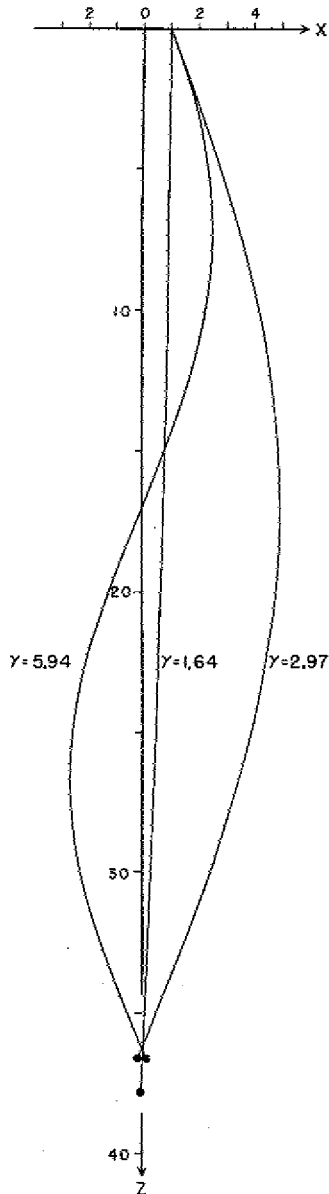


Fig. 17 - Theoretical x-z projections based on the median root interpretation for the cable system  $\lambda = 37.8$ ,  $w_f = 1352$

of a solution surface in a three-dimensional reaction space present obvious difficulties.

The results of this report should also serve as a considerable warning to those interested in studying the behavior of a cable towed in an arbitrary path. The fact that the dynamic boundary value problem can be non-unique poses several questions of both numerical and mathematical stability which should be closely examined.

#### ACKNOWLEDGMENTS

The author expresses his appreciation to Mr. John L. Bachman of the Ocean Structures Branch, Ocean Technology Division, for his assistance in designing and performing the experiment reported herein.

#### REFERENCES

1. Pode, L., "Tables for Computing the Equilibrium Configuration of a Flexible Cable in a Uniform Stream," DTMB Report 687, Mar. 1951
2. Wilson, B.W., "Characteristics of Anchor Cables in Uniform Ocean Currents," Texas A & M Research Foundation Technical Report No. 204-1, Apr. 1960
3. Skop, R.A., and O'Hara G.J., "The Static Equilibrium Configuration of Cable Arrays by Use of The Method of Imaginary Reactions," NRL Report 6819, Feb. 1969
4. Parsons, M.G., and Casarella, M.J., "A Survey of Studies on the Configuration of Cable Systems under Hydrodynamic Loading," Institute of Ocean Science and Engineering, The Catholic University of America, Themis Report 69-1, May 1969
5. Lamb, H., "Hydrodynamics," New York:Dover, 6th ed., 1945
6. Pode, L., "An Experimental Investigation of the Hydrodynamic Forces on Stranded Cables," DTMB Report 713, May 1950
7. Gay, S.M., "New Engineering Techniques for Application to Deep-Water Mooring," ASME Paper 66-Pet-31, Sept. 1966
8. Reid, R.O., "Dynamics of Deep-Sea Mooring Lines," Texas A & M Research Foundation Technical Report No. 204-5, July 1968
9. Strandhagen, A.G., and Thomas, C.F., "Dynamics of Towed Underwater Vehicles," U.S. Navy Mine Defense Laboratory Report 219, Nov. 1963
10. Margenau, H., and Murphy, G.M., "The Mathematics of Physics and Chemistry," Vol. 1, Princeton:Van Nostrand, 2d ed., 1956